Chapter 3
MAX-DOAS Measurements of ClO, SO_2 and NO_2 in the Mid-Latitude Coastal Boundary Layer and a Power Plant Plume

Chulkyu Lee[1,2], Young J. Kim[1], Hanlim Lee[1], and Byeong C. Choi[3]

Abstract Remote sensing techniques have been preferred for measurements of atmospheric trace gases because they allow direct measurement without pre- and/or post-treatment in the laboratory. UV–visible absorption measurement techniques have been used for ground-based remote sensing of atmospheric trace species. The multi-axis differential optical absorption spectroscopy (MAX-DOAS) technique, one of the remote sensing techniques for air quality measurement, uses scattered sunlight as a light source and measures it at various elevation angles by sequential scanning with a stepper motor. Ground-based MAX-DOAS measurements were carried out to investigate ClO, SO_2 and NO_2 levels in the mid-latitude coastal boundary layer from 27 May to 9 June, 2005, and SO_2 and NO_2 levels in fossil fuel power plant plumes from 10 to 14 January 2004. MAX-DOAS data were analyzed to identify and quantify ClO, SO_2 and NO_2 by utilizing their specific structured absorption features in the UV region. Differential slant column densities (dSCDs) for ClO, SO_2 and NO_2 were as high as 7.3×10^{14}, 2.4×10^{16} and 6.7×10^{16} molecules/cm^2 (with mean dSCDs of 2.3×10^{14}, 8.0×10^{15} and 1.2×10^{16} molecules/cm^2), respectively, at a 3° elevation angle in the coastal boundary layer during the measurement period. Based on the assumption that the trace gases were well mixed in the 1 km height of the boundary layer, estimates of the mean mixing ratios of ClO, SO_2 and NO_2 during the measurement period were 8.4 (±4.3), 296 (±233) and 305 (±284) pptv, respectively. MAX-DOAS measurement of the power plant plumes involved making vertical scans through multiple elevation angles perpendicular to the plume dispersion direction to yield cross-sectional distributions of ClO, SO_2 and NO_2 in the plume in terms of SCDs. Mixing ratios based on the estimated cross-sections of the plumes were 15.5 (ClO), 354 (SO_2) and 210 (NO_2) ppbv in the plumes of the fossil fuel power plant.

[1] *Advanced Environmental Monitoring Research Center (ADEMRC), Department of Environmental Science and Engineering, Gwangju Institute of Science and Technology (GIST), 1 Oryong-dong, Buk-gu, Gwangju 500-712, Republic of Korea*

[2] *Now at Institute of Environmental Physics and Remote Sensing, University of Bremen, Otto-Hahn-Allee 1, D-28334, Bremen, Germany*

[3] *Meteorological Research Institute, 460-18 Sindaebang-dong, Dongjak-gu, Seoul 156-720, Republic of Korea*

Y.J. Kim and U. Platt (eds.), *Advanced Environmental Monitoring*, 37–49.

Keywords: Air pollution, chlorine monoxide, DOAS, remote sensing

3.1 Introduction

Since the discovery of the ozone hole over Antarctica, halogen oxides have been of great environmental concern due to their ability to cause ozone depletion in the atmosphere (Farman et al., 1985; McElroy et al., 1986; Solomon et al., 1986). The importance of halogen chemistry for the tropospheric ozone budget was acknowledged following investigations of ozone depletion in the polar boundary layer (McElroy et al., 1999; Leser et al., 2003; Salawitch et al., 2006). Processes releasing halogens into the atmosphere and their effects on atmospheric chemistry have been the subject of a number of laboratory, field and modeling investigations (Schall and Heumann 1993; Mozurkewich 1995; Wayne et al., 1995; Sander and Crutzen 1996; von Glasow, et al., 2002; N. Bobrowski et al., 2003; Lee et al., 2005b; Salawitch 2006).

It is known that chlorine monoxide (ClO) plays a key role in processes leading to ozone loss in the troposphere and stratosphere. Gas-phase chlorine for ClO production in coastal areas is mostly released from sea salt through heterogeneous reactions (Fan and Jacob 1992; Sander and Crutzen 1996; Vogt et al., 1996). Enhanced levels of ClO in the boundary layer associated with ozone destruction have been observed over salt lakes (Stutz et al., 2002), in the polar boundary layer (Tuckermann et al., 1997), and in volcanic plumes (Lee et al., 2005b). However, there is little information on ClO and its effects on ozone depletion in the mid-latitude coastal boundary layer. Although other halogen species (e.g. BrO and IO) have been measured in coastal areas (Leser et al., 2003; Saiz-Lopez and Plane 2004; Saiz-Lopez et al., 2004), few direct measurements of ClO have been reported.

Anthropogenic SO_2 and NO_2 emissions are chemically converted to sulfuric and nitric acids in the atmosphere in the gaseous and aqueous phases. When these acids precipitate, damage is caused to buildings and ecosystems, particularly in areas where soils lack sufficient alkalinity to buffer these acids. The related formation of sulfate aerosols can increase the incidence of human respiratory ailments and associated mortality. Most measurements of these species emitted from the stack of an industrial facility such as a power plant can be performed using direct sampling methods, in situ monitoring techniques, or remote sensing techniques. The direct sampling methods are based on the collection of air samples by an appropriate container, with subsequent analysis in the laboratory. These techniques usually offer high sensitivity and selectivity, but have disadvantages in requiring real-time and continuous monitoring. Problems may also arise owing to alterations of gas composition caused by adsorption and desorption processes at the inner surface of the collecting container. In situ real-time monitoring techniques are often less sensitive and selective than direct sampling methods, though they offer the advantage of real-time measurements. Furthermore, direct sampling and in situ sampling around the outlet of an industrial stack is often impractical and hazardous.

Ultraviolet–visible absorption spectroscopy of remote sensing techniques has mostly been applied to the measurement of atmospheric trace species. The strength of this technique lies in the absence of wall losses, good specificity, and the potential for real-time measurements. In particular, the first property makes spectroscopic techniques especially well-suited for the detection of unstable species like OH radicals (Dorn et al., 1988), nitrate radicals (Platt et al., 1981) and halogen radicals (Tuckermann et al., 1997; Wagner et al., 1998; Stutz et al., 2002; Saiz-Lopez and Plane 2004; Saiz-Lopez et al., 2004). Since the 1970s, Differential optical absorption spectroscopy (DOAS) has been considered a powerful tool for the detection of atmospheric trace species on a real-time basis. The DOAS technique can gather sensitive measurements of several trace species simultaneously (Platt et al., 1981; Hausmann and Platt 1994; Tuckermann et al., 1997; Wagner et al., 1998; Hebestreit et al., 1999; Stutz et al., 2002; Saiz-Lopez and Plane 2004; Saiz-Lopez et al., 2004; Lee et al., 2005b).

Scattered sunlight in the near ultraviolet–visible spectral ranges has been employed for the analysis of atmospheric trace species by ground-based DOAS. This application is also called 'passive' absorption spectroscopy in contrast to 'active' spectroscopy using artificial light sources. Scattered sunlight DOAS measurements yield slant column densities of the respective absorbers. Most measurements have been conducted with zenith-looking instruments because the radiative transfer modeling necessary for the determination of vertical column densities is best understood for zenith-scattered sunlight. The multi-axis differential optical absorption spectroscopy (MAX-DOAS) technique is a passive DOAS technique using scattered sunlight from several viewing directions in addition to conventional zenith pointing. This ground-based instrument receives scattered sunlight from different viewing directions with several telescopes or by changing the viewing direction of a single telescope, thus collecting spatial information of atmospheric trace species. Measurement using low telescope elevation angles emphasizes the absorption path in the lowermost atmospheric layers and exhibits enhanced sensitivity for absorbers in the boundary layer, while photons received from the zenith-looking telescope have traveled a relatively long path in the stratosphere and a comparatively short path in the troposphere.

MAX-DOAS measurements were carried out to investigate ClO, SO_2 and NO_2 levels in the mid-latitude coastal boundary layer and in plumes of a fossil fuel power plant. Results concerning the levels of ClO, SO_2 and NO_2 and their diurnal variations in the mid-latitude coastal boundary layer are presented here. We also provide data on the levels and distribution of ClO, SO_2 and NO_2 in the plumes of a fossil fuel plant.

3.2 Measurement

Our sequential MAX-DOAS system essentially consists of a small aluminium box containing a miniature spectrograph and a telescope. The miniature spectrograph (OceanOptics USB2000, cross Czerny-Turner type, $1/f = 4$)

consists of a grating (2,400 grooves/mm) yielding spectral coverage between 289 and 431 nm (at a 0.7 nm FWHM spectral resolution) and a CCD detector (2,048 pixels with a 14 μm center-to-center spacing) (Lee et al., 2005b). The MAX-DOAS box was attached directly to a stepper motor, allowing sequential measurement of scattered sunlight at various elevation angles between 0° and 90° above the horizon. Dark current and offset signals were also recorded during the nighttime. The MAX-DOAS system was operated using the DOASIS software developed by the Institute of Environmental Physics, University of Heidelberg, Germany.

MAX-DOAS measurements of ClO, SO_2 and NO_2 in the mid-latitude coastal boundary layer were carried out at the Korea Global Atmosphere Watch Observatory (KGAWO) (36.54° N, 127.12° E) located on Anmyeon island off the west coast of Korea. Several resorts are located on Anmyeon island, and there is increased traffic around nearby resorts on weekends. The KGAWO station is 230 m from the west coast of Anmyeon island, and has occasionally been affected by the long-range transport of pollutants from the Asian continent. MAX-DOAS measurements were made on the roof of the KGAWO building (43 m above sea level) during the daytime from 27 May to 9 June 2005. The viewing azimuth angle of the MAX-DOAS telescope was 340° (0° indicates a true north direction), looking to the sea. Scattered sunlight signals were recorded at telescope elevation angles of 3, 6, 10, 20 and 90°. Each measurement sequence took about 10–20 min. Measured MAX-DOAS spectra were analyzed to identify and quantify levels of ClO, SO_2 and NO_2 using their specific structured absorption features in the ultraviolet region (Platt 1994). In situ gas analyzers measuring SO_2, O_3 and NO_x were also installed 10 m above the ground at KGAWO. Meteorological data that included wind speed and direction were also collected by an automatic weather station (AWS) installed 40 m above ground level at KGAWO. Measurements of SO_2 and NO_2 in the plumes emitted from a power plant were made from 10 to 14 January 2004 at a fossil fuel power plant in the west of Korea. Telescope elevation angles of 2, 5, 10, 20, 30, 40, 50, 60, 70, 80 and 90° above the horizon were used to scan the plume, resulting in cross-sectional measurements of the plume. Each measurement sequence of the plume cross-section took about 15–25 min. Mercury lamp line peaks were also recorded on 29 May and 9 June 2006 to check for any spectral shifts of the spectrograph and ensure its wavelength calibration.

Spectra taken by the MAX-DOAS system were calibrated using mercury lamp line peaks corrected for dark current and electric offset signal by subtracting the dark current and offset signals recorded. Then the calibrated DOAS spectra were calibrated again by fitting them to the solar reference file. Slant column densities (SCDs) of ClO, SO_2 and NO_2 were derived from the calibrated DOAS spectra using the WinDOAS V2.10 software package (Van Roozendael and Fayt 2001). Scattered sunlight is highly structured due to solar Fraunhofer lines. These structures were removed by including the Fraunhofer reference spectrum (FRS) in the fitting procedure. The scattered sunlight spectrum taken at an elevation angle of 90° (zenith direction) around noon

(local time) on a cloudless day was used as the FRS, where only negligible background trace gas absorption was present. To compensate for the ring effect (Fish and Jones 1995; Chance and Spurr 1997), which represents the filling-in (reduction of the observed optical densities) of Fraunhofer lines, a 'ring spectrum' was calculated from the FRS. In addition to a polynomial order fit to remove broad band structures, the FRS, ring spectrum and literature sources of absorption cross-section spectra were simultaneously fitted to the scattered sunlight spectra using the nonlinear least square method (Stutz and Platt 1996). High-resolution reference absorption spectra were obtained from previous studies (Greenblatt et al., 1990; Simon et al., 1990; Vandaele et al., 1997; Wilmouth et al., 1999; Meller and Moortgat 2000; Bogumil et al., 2003). The specifications for the evaluation of ClO, SO_2 and NO_2 are summarized in Table 3.1. Figure 3.1 shows an example of a MAX-DOAS spectrum evaluation for ClO in the coastal boundary layer. All reference absorption cross-section spectra used for the evaluation of ClO, SO_2 and NO_2 were convoluted with the instrumental function to match the spectral resolution of the MAX-DOAS system used in this study.

For MAX-DOAS measurements in the coastal area, the retrieved SCDs from MAX-DOAS spectra recorded at a 90° elevation angle were subtracted from those obtained at other elevation angles during each scanning sequence. This procedure yields differential SCDs (DSCDs) (= SCD[α, θ] − SCD[90°, θ]), where α is an elevation angle and θ is a solar zenith angle, and removes absorptions by trace gases in the stratosphere (Leser et al., 2003; Friedeburg et al., 2005).

Table 3.1 Specifications for the MAX-DOAS spectrum evaluation for ClO, NO_2 and SO_2

Molecule	Wavelength range, nm	Polynomial order	Cross-sections included in the fitting procedure
ClO	302.5–316	3	ClO[a], BrO[b], SO_2[c], HCHO[d], NO_2[e], O_3[f], Ring[g], FRS[h]
SO_2	303.5–316	3	ClO[a], SO_2[c], BrO[b], NO_2[e], O_3[f], Ring[b], FRS[c]
NO_2	399–418	3	NO_2[e], O_4[i], O_3[f], Ring[g], FRS[h]

The cross-sections of NO_2, O_3 and SO_2 were I_0-corrected (Aliwel et al., 2002)
[a] ClO at 300 K (Simon et al., 1990)
[b] BrO at 298 K (Wilmouth et al., 1999)
[c] SO_2 at 293 K (Bogumil et al., 293)
[d] HCHO at 298 K (Meller and Moortgat 2000)
[e] NO_2 at 294 K (Vandaele et al., 1997)
[f] Two O_3 cross-sections obtained at 223 K and 241 K were included in the fitting routine.
[g] Ring spectrum
[h] Fraunhofer reference spectrum
[i] O_4 at 296 K (Greenblatt et al., 1990)

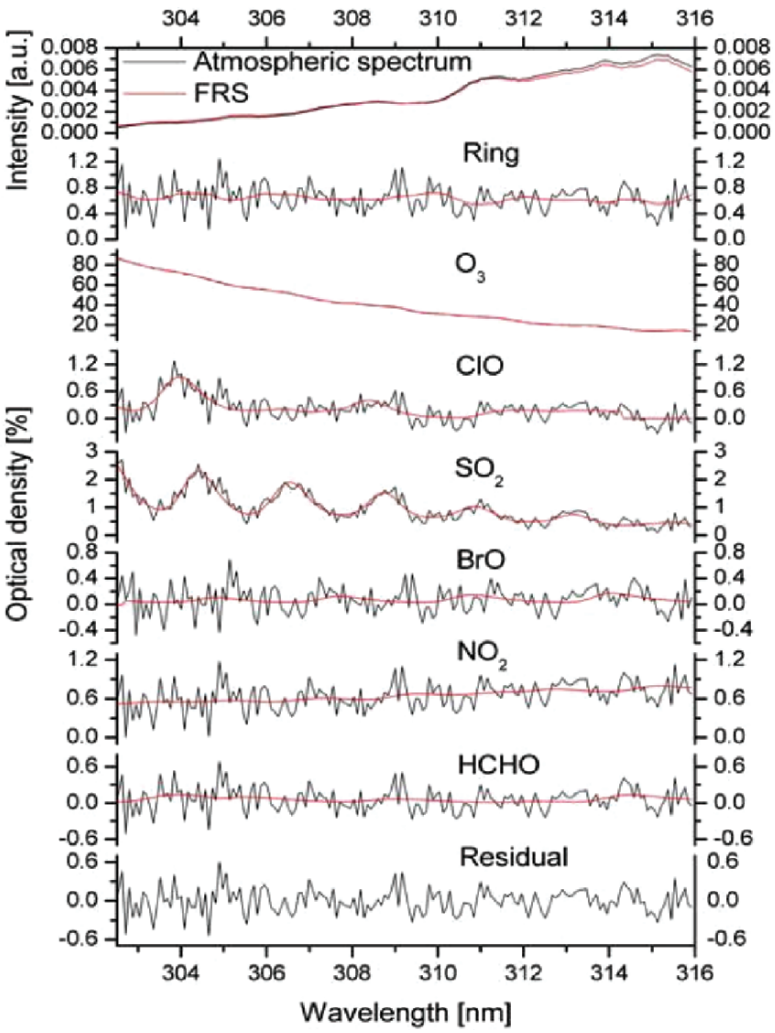

Fig. 3.1 An evaluation example of a ClO SCD from the MAX-DOAS spectrum taken at a 3° elevation angle at 16:12 on 5 June 2005 (LT)

3.3 Results

3.3.1 ClO, SO_2 and NO_2 in the Mid-Latitude Coastal Boundary Layer

Figure 3.2 shows the temporal variations of DSCDs for ClO, SO_2 and NO_2 measured at KGAWO during the measurement period. The mean DSCDs of ClO, SO_2 and NO_2 at a 3° elevation angle were 2.3 (±1.2) × 10^{14}, 8.0 (±6.3) × 10^{15} and

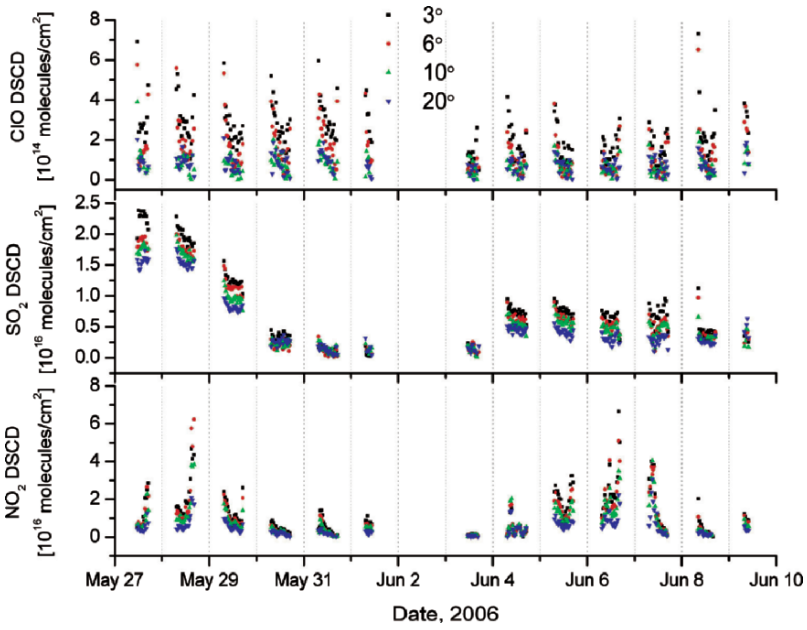

Fig. 3.2 ClO, SO_2 and NO_2 differential slant column densities (DSCD) at different elevation angles determined by the MAX-DOAS system. The date at the tic-mark denotes 0:00 h (local time) for the given day

1.2 (±1.1) × 10^{16} molecules/cm^2, with maximum values of 7.3 × 10^{14}, 2.4 × 10^{16} and 6.7 × 10^{16} molecules/cm^2, respectively.

The mean DSCDs of ClO, SO_2 and NO_2 observed during the measurement period can be converted to a mixing ratio. Mixing ratios can be calculated in the following manner on the assumption that the change of air density was negligible in the lowest 1 km of the atmosphere:

$$M = \frac{DSCD}{dAMF} \cdot \frac{1}{z} \tag{1}$$

where M is the mixing ratio, z is the height of the trace gas layer, and dAMF is a differential air-mass factor (AMF[α = 3°])−AMF[α = 90°]). The AMFs in this study were calculated using the Monte Carlo radiative transfer model described in von Friedeburg et al. (2002), which included multiple Rayleigh and Mie scattering, surface albedo, refraction, and full spherical geometry. Calculated dAMFs were 10.2 and 14.5 for 304 nm (for ClO and SO_2) and 412 nm (for NO_2) wavelengths, respectively, assuming a 30° solar zenith angle, 5% ground albedo, and a pure Rayleigh case for the troposphere. The mixing ratios converted from the DSCDs of ClO, SO_2 and NO_2 observed during the measurement period are shown in Fig. 3.3. The mean mixing ratios for ClO, SO_2 and NO_2 were 8.4 (±4.3), 296 (±233) and 305 (±284) pptv, respectively, if it is assumed that the trace gases were well-mixed within the 1-km height of the boundary layer.

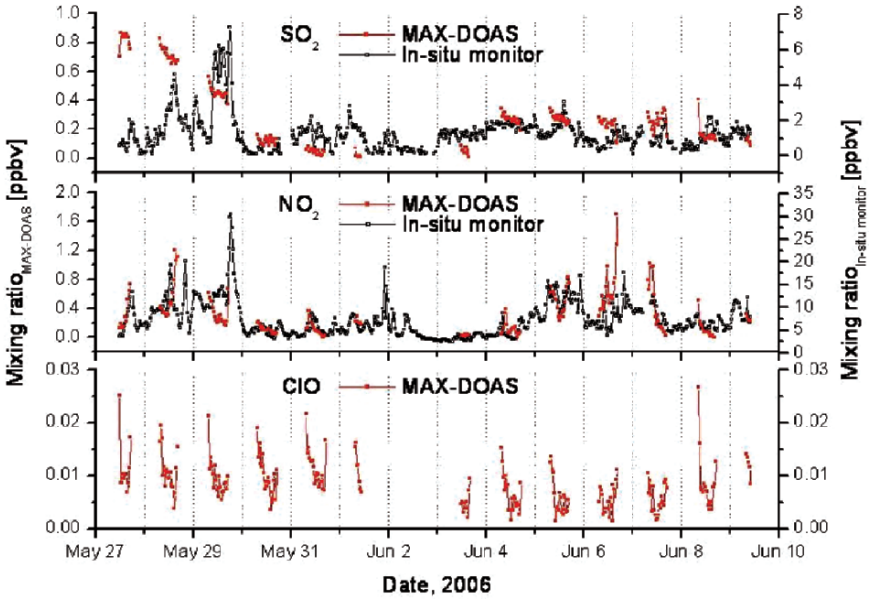

Fig. 3.3 Mixing ratios of SO_2 and NO_2 determined by the MAX-DOAS system and in situ monitors. ClO mixing ratios were determined by the MAX-DOAS system. The date at the tic-mark denotes 0:00 h (local time) for the given day

As shown in Figures 3.2 and 3.3, the diurnal variation of DSCD for ClO shows maxima in the morning and evening, and a minimum around noon. These changes have been predicted by a halogen chemistry model in the marine boundary layer (von Glasow et al., 2002). This feature can be explained by the difference in the photolysis spectra of O_3 and ClX, in which ClX is photolyzed by longer wavelengths of sunlight than O_3 (von Glasow et al., 2002). The major source of gas-phase chlorine in the coastal area is the release of species such as Cl_2 and BrCl from sea-salt aerosol, following the uptake of the gas phase and subsequent aqueous-phase reactions of hypohalous acids (HOX, where X = Br, Cl, I) (Vogt et al., 1996; Saiz-Lopez et al., 2004). The formation of $ClNO_2$ and X_2 can proceed by uptake of N_2O_5 formed at night by combination of NO_3 and NO_2, leading to an accumulation of these species before sunrise. They are photolyzed by sunlight to release Cl that subsequently participates in gas-phase catalytic reaction cycles (Fan and Jacob 1992; Vogt et al., 1996). This effect is more pronounced with higher levels of NO_x. The reactive halogen species in the troposphere are mainly removed by their reaction with proxy radicals, such as HO_2. The HO_2 mixing ratios are sufficiently high during the day to reduce the DSCD of ClO, resulting in the noon minimum. The relative lack of shorter wavelengths of sunlight at higher solar zenith angles leads to an increase in the DSCD of ClO, which produces the morning and evening peaks. Moreover, the high DSCD of ClO in the morning and evening could be the result of a higher relative humidity during those hours.

Table 3.2 SO_4^{2-}/SO_2 ratios determined for each PM1 sample collected for 24 h

	May 27	May 29	May 30	May 31	June 04	June 05	June 06	June 07	June 08
SO_4^{2-}/SO_2 ratio	6.05	1.36	5.98	0.82	1.37	0.76	1.77	1.41	2.74

NO_2 plays an important role in atmospheric chemistry by acting as a catalyst in the photochemical production of O_3. If halogens are present, NO_x mixing ratios are further reduced by reactions of NO_2 with ClO, yielding XNO_3 (Platt and Hönninger 2003). The initial high mixing ratios of NO_2 enhance chlorine activation, resulting in increases of ClO and an upward shift of O_3 destruction rates (von Glasow et al., 2002). The probabilities and rates of heterogeneous reactions for the release of reactive halogens increase with a higher concentration of acids (Fan and Jacob 1992).

The mixing ratios of NO_2 and SO_2 measured by the MAX-DOAS system and in situ monitors are plotted in Fig. 3.3. Relatively high NO_2 and SO_2 levels were observed during two periods: 27–29 May 2005, and 4–7 June 2005. The discrepancy in SO_2 and NO_2 trends between the MAX-DOAS system and in situ monitors during the first event period of 27–29 May 2005 could be due to the inhomogeneity of the air masses. The major difference between the MAX-DOAS system and in situ instruments is the fact that the passive MAX-DOAS system relies on the sun as its light source. Therefore, instrumental differences associated with measurement principles (i.e. line-integrating versus point measurement) need to be considered for an evaluation of MAX-DOAS performance (Lee et al., 2005a). The KGAWO site is occasionally affected by the long-range transport of pollutants from the Asian continent. The air mass transported from the Asian continent could be in the upper part of the boundary layer over the KGAWO site, and may have spread horizontally and towards the ground during the first event period. It is believed that an aged air mass had an impact during the first event period since the NO concentration during the first event period was lower than that recorded during the second period. This is supported by satellite images indicating the transport of an air mass from the Asian continent, and by high SO_4^{2-}/SO_2 ratios of PM1 samples collected by an URG PM1 sampler, as summarized in Table 3.2. In addition to the long-range transport of pollutants, local sources of pollution such as increased traffic around nearby resorts on weekends could have contributed to the high concentrations of NO_2 and SO_2 during the first measurement period, particularly on 29 May 2006. The increased concentrations of NO_2 and SO_2 observed during the second period on a weekend could be attributed to local sources.

3.3.2 ClO, SO_2 and NO_2 Measurement in the Plumes of a Fossil Fuel Power Plant

ClO, SO_2 and NO_2 were detected in each scan through the plume. The cross-sectional distribution of slant column densities was characterized by maximum SCDs in the viewing direction (elevation angle) toward the center of the plume at

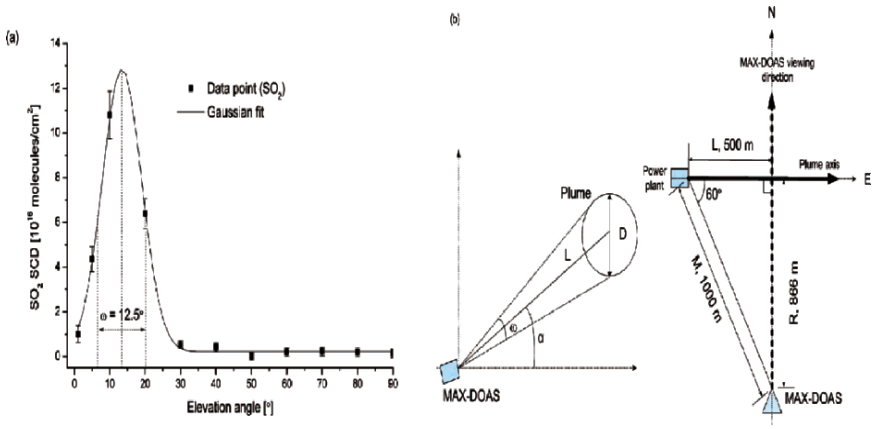

Fig. 3.4 (**a**) Cross-section of the fossil fuel power plant plume for SO_2, and (**b**) MAX-DOAS measurement geometry

any elevation angle, as shown in Fig. 3.4(a). SCDs measured during the measurement period were as high as 1.2×10^{16}, 1.6×10^{17} and 2.2×10^{17} molecules/cm^2 in the center of the plume for ClO, SO_2 and NO_2, respectively.

A cross-section of the plume was estimated to determine mixing ratios of species measured from the plume (see Fig. 3.4[a]). After the plume cross-section (assumed to be circular) was fitted with a Gaussian distribution, the plume diameter, D, was determined from the width, ω, (full width at half maximum) as: $D \approx L \times \omega \times \cos(\varphi)$, where φ is the observation azimuth angle. The plume width, ω, was 13.2° for ClO, 12.5° for SO_2 and 15.2° for NO_2 (based on data collected on 11 January 2004 and $\varphi \approx 0°$ (see Fig. 3.4[b]), which correspond to plume diameters of ≈ 200 (±30), 190 (±30) and 230 (±31) m for ClO, SO_2 and NO_2, respectively. Based on the measured maximum SCD (ClO ≈ 8.3×10^{15}, $SO_2 \approx 1.8 \times 10^{17}$ and $NO_2 \approx 1.3 \times 10^{17}$ molecules/cm^2), the calculated mixing ratios (= SCD × cos(0°)/D) were ~15.5, ~354 and ~210 ppbv for ClO, SO_2 and NO_2, respectively. The SO_2 mixing ratio was above the standard established for air pollutants emitted from a power plant in Korea (150 ppbv for SO_2), while the mixing ratio of NO_2 was below the standard (250 ppbv for NO_2).

3.4 Conclusion

While MAX-DOAS is a new and emerging technique based on the scattered sunlight DOAS method, the ground-based MAX-DOAS system allows the determination of relatively precise levels of absorbers in the boundary layer using simple instrumentation. In this study, MAX-DOAS proved to be successful in applications that monitored trace gases in power plant plumes and ambient air. ClO, SO_2 and NO_2 have been directly observed in the mid-latitude coastal

boundary layer by the MAX-DOAS technique. We demonstrated that the MAX-DOAS technique is capable of measuring trace species in the boundary layer with high sensitivity. The diurnal behavior of ClO was consistent with a source based on the heterogeneous processing of sea-salt aerosol. The ClO level was as high as ~27 pptv (with a mean of 8.4 pptv) during the measurement period, and is comparable to ClO levels of up to 15 pptv in the boundary layer over the Great Salt Lake (Stutz et al., 2002) and 30 pptv in the polar boundary layer (Tuckermann et al., 1997). Mean SO_2 and NO_2 levels observed during the measurement period were 296 (±233) and 305 (±284) ppbv, respectively. High SO_2 and NO_2 concentrations measured during the two event periods might have an effect on atmospheric halogen chemistry through reactive halogen release processes by the attack of strong acids on sea-salt aerosols, and through reducing processes by the reaction of ClO with NO_2 (Platt and Hönninger 2003). The ClO emitted from sea salt as a consequence of recycling processes has a long atmospheric lifetime of up to several days (Barrie and Platt 1997; Tuckermann et al., 1997; Platt and Hönninger 2003), and may therefore, play an important role in atmospheric chemistry. Further observations are required to quantify the seasonal effect of halogen species originating from sea-salt aerosol on tropospheric chemistry (in particular, ozone chemistry) of the mid-latitude region.

The ground-based MAX-DOAS system has also proven to be suitable for the measurement of ClO, SO_2 and NO_2 emissions from a power plant by scanning the plume from fixed positions. Mixing ratios calculated from cross-sectional distributions of ClO, SO_2 and NO_2 in fossil fuel power plant plumes were ~15.5, ~354 and ~210 ppbv, respectively. The emission strength can be determined if the wind speed is provided. The ground-based MAX-DOAS technique is considerably cheaper and simpler than other available remote sensing methods, and shows great potential for the routine, remote monitoring of industrial stacks. It is also suitable for studies of the transport, dispersion and chemistry of plumes.

Acknowledgements This work was supported by the Korea Science and Engineering Foundation through the Advanced Environmental Monitoring Research Center (ADEMRC) of the Gwangju Institute of Science and Technology (GIST).

References

Barrie L. and Platt, U. (1997), Artic tropospheric chemistry: An overview, *Tellus*, 49B, 450–454.

Bobrowski N., Hönninger G., Galle B., and Platt U. (2003), Detection of bromine monoxide in a volcanic plume, *Nature*, 423, 273–276.

Bogumil K., Orphal J., Homann T., Voigt S., Spietz P., Fleischmann O.C., Vogel A., Hartmann M., Bovensmann H., Frerik J., and Burrows J.P. (2003), Measurements of molecular absorption spectra with the SCIAMACHY pre-flight model: Instrument characterization and reference data for atmospheric remote sensing in the 230–2380 nm region, *J.Photoch. Photobiol. A*, 157, 167–184.

Chance K.V. and Spurr R.J.D. (1997), Ring effect studies: Rayleigh scattering, including molecular parameter for rotational Raman scattering, and the Fraunhofer spectrum, *Appl. Optics*, 36, 5224–5230.

Fan S.-M. and Jacob D.J. (1992), Surface ozone depletion in Artic spring sustained by bromine reaction on aerosols, *Nature*, 359, 522–524.

Farman J.C., Gardiner B.G., and Shaklin J.D. (1985), Large losses of total ozone in Antarctica reveal seasonal ClO_x/NO_x interaction, *Nature*, 315, 207–210.

Fish D.J. and Jones R.L. (1995), Rotational Raman scattering and the ring effect in zenith-sky spectra, *Geophys. Res. Lett*., 22, 811–814.

Greenblatt G.D., Orlando J.J., Burkholder J.B., and Ravishankara A.R. (1990), Absorption measurements of oxygen between 330 and 1140 nm, *J. Geophys. Res*., 95, 18, 577–582.

Hausmann M. and Platt U. (1994), Spectroscopic measurement of bromine oxide and ozone in the high Arctic during polar sunrise experiments 1992, *J. Geophys. Res*., 99, 25, 399–413.

Hebestreit K., Stutz J., Rosen D., Matveiv V., Pelg M., Luria M., and Platt U. (1999), DOAS measurements of tropospheric bromine oxide in mid-latitudes, *Science*, 283, 55–57.

Hönninger G., von Friedeburg C., and Platt U. (2004), Multi axis differential optical absorption spectroscopy (MAX-DOAS), *Atmos. Chem. Phys*., 4, 231–254.

Lee C., Choi Y.J., Jung J.S., Lee J.S., Kim Y.J., and Kim, K.H. (2005a), Measurement of atmospheric monoaromatic hydrocarbons using differential optical absorption spectroscopy: Comparison with on-line gas chromatography measurements in urban air, *Atmos. Environ*., 39, 2225–2234.

Lee C., Kim Y.J., Tanimoto H., Bobrowski N., Platt U., Mori T., Yamamoto K., and Hong C.S. (2005b), High ClO and ozone depletion observed in the plume of Sakurajima volcano, *Geophys. Res. Lett*., 32, DOI 10.1029/2005GL023785.

Leser H., Hönninger G., and Platt U. (2003), MAX-DOAS measurements of BrO and NO_2 in the marine boundary layer, *Geophys. Res. Lett*., 30, DOI 10.1029/2002GL015811.

Marchand M., Bekki S., Lefèvere F., Hauchecorne A., Godin-Beckmann S., and Chipperfield M.P. (2004), Model simulations of the northern extravortex ozone column: Influence of past changes in chemical composition, *J. Geophys. Res*., 109, DOI 10.1029/2003JD003634.

McElroy C.T., McLinden C.A., and McConnell J.C. (1999), Evidence for bromine monoxide in the free troposphere during the Arctic polar sunrise, *Nature*, 397, 338–341.

McElroy M.B., Salawitch R.J., Wofsy C.S., and Logan J.A. (1986), Reductions of Antarctic ozone due to synergistic interactions of chlorine and bromine, *Nature*, 321, 759–762.

Meller R. and Moortgat G.K. (2000), Temperature dependence of the absorption cross sections of formaldehyde between 223 and 323 K in the wavelength range 225–375 nm, *J. Geophys. Res*., 105, 7089–7101.

Mozurkewich M. (1995), Mechanisms of the release of halogen atom sea-salt particles by free radical reactions, *J. Geophys. Res*., 100, 14, 199–207.

Platt U. (1994), Differential optical absorption spectroscopy (DOAS). In M.W. Sigrist (Eds.), *Monitoring by Spectroscopic Techniques*, Wiley, New York, pp. 27–84.

Platt U. and Hönninger G. (2003), The role of halogen species in the trosposphere, *Chemosphere,* 52, 325–338.

Salawitch R.J. (2006), Atmospheric chemistry: Biogenic bromine, *Nature*, 439, 275–277.

Sander R. and Crutzen P.J. (1996), Model study indicating halogen activation and ozone destruction in polluted air masses transported to the sea, *J. Geophys. Res*., 101, 9121–9138.

Schall C. and Heumann K. (1993), GC determination of volatile organoiodine and organobromine compounds in seawater and air samples, *Fresen. J. Anal. Chem*., 346, 717–722.

Saiz-Lopez A. and Plane J.M.C. (2004), Novel iodine chemistry in the marine boundary layer, *Geophys. Res. Lett*., 31, DOI 10.1029/2003GL019215.

Saiz-Lopez A., Plane J.M.C., and Shillito J.A. (2004), Bromine oxide in the mid-latitude marine boundary layer, *Geophys. Res. Lett*., 31, DOI 10.1029/2003GL018956.

Simon F.G., Schneider W., Moortgat G.K., and Burrows J.P. (1990), A study of the ClO absorption cross-section between 240 and 310 nm and the kinetics of the self-reaction at 300 K, *J. Photoch. Photobiol. A*, 55, 1–23.

Solomon S. (1990), Progress towards a quantitative understanding of Antarctic ozone depletion, *Nature*, 347, 347–354.

Solomon S., Garcia F.S., Rowland F.S., and Wuebbles D.J. (1986), On the depletion of Antarctic ozone, *Nature*, 321, 755–758.

Stutz J. and Platt U. (1996), Numerical analysis and error estimation of differential optical absorption spectroscopy measurements least-squares methods, *Appl. Optics,* 35, 6041–6053.

Stutz J., Ackermann R., Fast J.D., and Barrie L. (2002), Atmospheric reactive chloride and bromine at the Great Salt Lake, Utah, *Geophys. Res. Lett*., 29, DOI 10.1029/2002GL014812.

Tuckermann M., Ackermann R., Gölz C., Lorezen-Schmidt H., Senne T., Stutz J., Trost B., Unold W., and Platt U. (1997), DOAS-observation of halogen radical-catalysed arctic boundary layer ozone destruction during the ARCTOC-campaigns 1995 and 1996 in Ny-Ålesund, Spitshergen, *Tellus*, 49B, 533–555.

Vandaele A.C., Hermans C., Simon P.C., Carleer M., Colin R., Fally S., Mérienne M.-F., Jenouvrier A., and Coquart B. (1997), Measurements of the NO_2 absorption cross-section from 42000 cm^{-1} to 10000 cm^{-1} (238–1000 nm) at 220 K and 294 K, *J. Quant. Spectrosc. Radiative. Transf*., 59, 171–184.

Van Roozendael M. and Fayt C. (2001), *WinDOAS 2.1 Software User Mannual*. (Uccle, IASB/BIRA).

Vogt R., Crutzen P.J., and Sander R. (1996), A mechanism for halogen release from sea-salt aerosol in the remote marine boundary layer, *Nature*, 383, 327–330.

Wagner T. and Platt U. (1998), Satellite mapping of enhanced BrO concentrations in the troposphere, *Nature*, 395, 486–490.

von Friedeburg C., Hönninger G., and Platt U. (2005), Multi-axis-DOAS measurements of NO_2 during the BAB II motorway emission campaign, *Atmos. Environ*., 39, 977–985.

von Glasow R., Sander R., Bott A., and Crutzen P.J. (2002), Modelling halogen chemistry in the marine boundary layer 1. Cloud-free MBL, *J. Geophys. Res*., 107(D17), DOI 10.1029/2001JD000942.

Wayne R.P., Poulet G., Biggs P., Burrows J.P., Cox R.A., Crutzen P.J., Hayman G.D., Jenkin M.E., Bras G.L., Moortgat G.K., Platt U., and Schindler R.N. (1995), Halogen oxides: Radicals, sources and reservoirs in the laboratory and in the atmosphere, *Atmos. Environ*., 29, 2677–2881.

Wilmouth D.M., Hanisco T.F., Donahue N.M., and Anderson J.G. (1999), Fourier transfer ultraviolet spectroscopy of the A2P3/2 X2P3/2 transition of BrO, *J. Phys. Chem. A*, 103, 8935–8945.